Rev. Adv. Mater. Sci. 43 (2015) 6-12

TEXTURE EVOLUTION OF NANOCRYSTALLINE NICKEL DURING PACK ROLLING

H.T. Ni[1], J. Zhu[1] and X.Y. Zhang[2]

[1]College of Materials and Chemical Engineering, Chongqing University of Arts and Sciences,Yongchuan, Chongqing 402160, China
[2]College of Materials Science and Engineering, Chongqing University, Chongqing 400044, China

Received: June 08, 2015

Abstract. The texture evolution of electrodeposited nanocrystalline nickel with an initial grain size of 20 nm during pack rolling is quantitatively investigated. For both the roll-bonding side and non-roll-bonding side, the volume fractions of {001}<100> and {001}<110> components decrease with increasing equivalent strain, whereas those of {110}<001>, {110}<1$\bar{1}$2>, {112}<110>, and {123}<634> components increase. This phenomenon is different from the texture evolution of conventional single-sheet rolled nanocrystalline nickel. However, the roll-bonding side and non-roll-bonding side behave quite differently. The deformation texture in the roll-bonding side at a high strain is characterized by the presence of strong {110}<001>, {110}<1$\bar{1}$2>, {112}<110>, and {123}<634> components, whereas a significant decrease in the {001}<100> and {001}<110> components. A cubic component having a volume fraction of 8% remains found in the non-roll-bonding side for the sample deformed to the largest strain of ε_{VM}=0.611. Detailed analysis suggests such a remnant of the original cube component can be primarily attributed to partial dislocation slip and grain coarsening.

1. INTRODUCTION

Deformation mechanism and mechanical property of nanocrystalline (NC) metals have received much attention in recent decades. With the help of molecular-dynamics simulation, Yamakov et al. have shown a deformation-mechanism map for NC metals [1]. Such map captures the transition from a dislocation-based to a grain-boundary-based deformation mechanism and the related mechanical behaviours with decreasing grain size. Based on different deformation mechanisms, Meyers et al. have reviewed numerous aspects of mechanical behavior for NC metals, with emphasis on their constitutive response and on the fundamental physical mechanisms [2]. The dependence of deformation mechanism on the grain size, grain boundary-mediated deformation in smaller grain size and dislocation-mediated deformation in larger grain size, is well documented [3-5]. Besides grain size dependence of plastic deformation, the dependence of deformation structure and mechanical property on grain orientation is also noted [6]. They have revealed that mechanical property of NC metals could be improved by the use of special columnar grain geometry. In particular, it should be pointed out that effects of texture on the grain size dependence of mechanical property in metals were proposed long ago [7,8]. These effects of preferred orientation will be particularly important in non-cubic metals, due to their limited slip systems. As we know, the texture of a material is the basis of its anisotropic behavior. The texture development could be used to get an insight into the elementary mechanisms which are responsible for plastic deformation and mechani-

Corresponding author: X.Y. Zhang, e-mail: kehen888@163.com

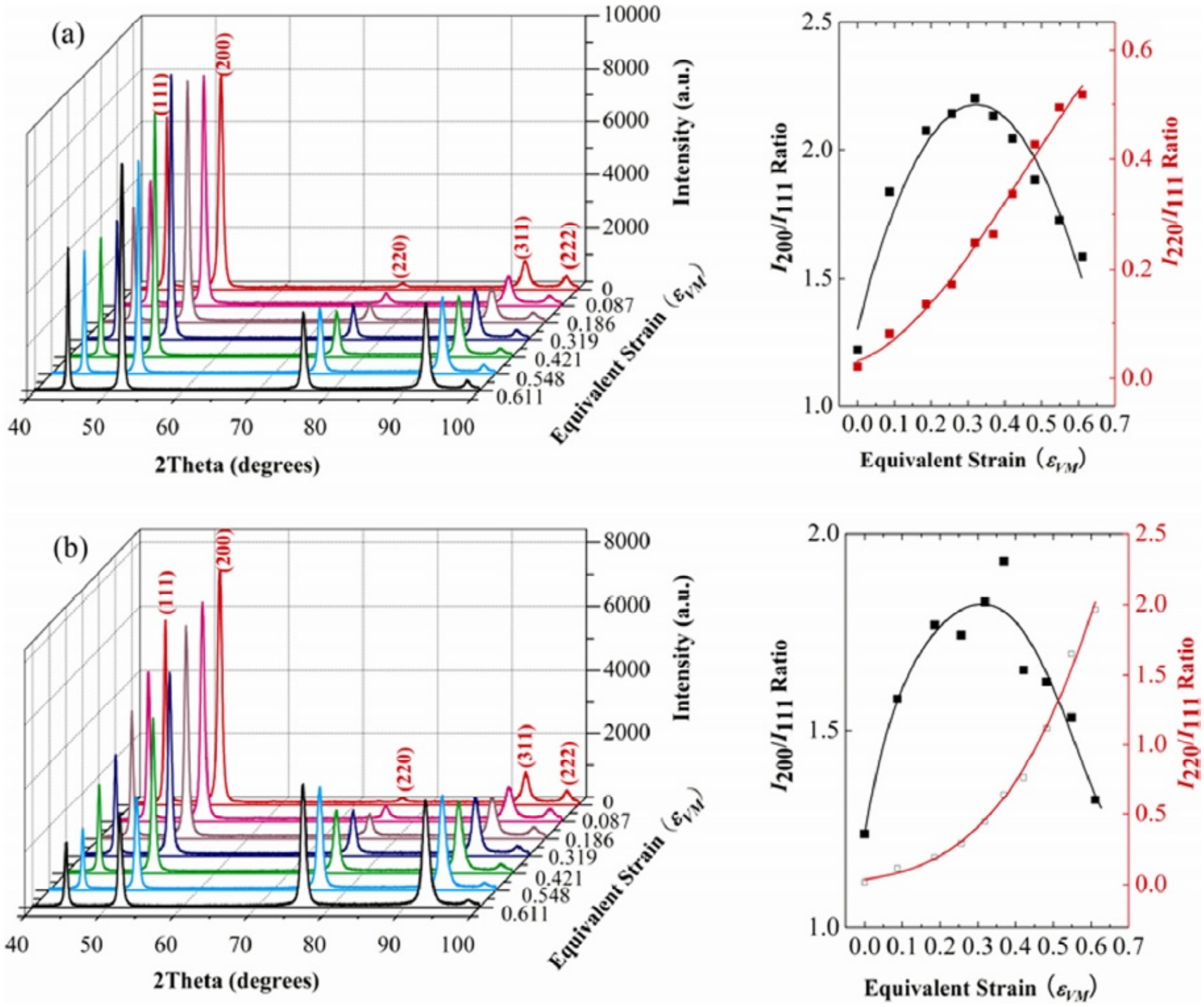

Fig. 1. XRD patterns for the (a) side NR and (b) side R of deformed nanocrystalline nickel at various stains. The corresponding (200)/(111) and (220)/(111) diffraction intensity rations (I_{200} / I_{111} and I_{220} / I_{111}) with increasing strain are shown in the right side.

cal behavior. From the findings attained so far, the absence of deformation texture in NC metals indicates that grain boundary (GB) sliding and grain rotation take place along with the dislocation-based plasticity [9,10]. Moreover, previous studies have shown that grain size has a crucial influence on the orientation changes during plastic deformation [11]. Thus, it is still an open issue on the deformation induced texture development in NC metals.

Similar to what is known for conventional metals, the main texture components commonly found in the rolled face-centered cubic (FCC) NC metals include the following types: {001}<100> (cube texture), {110}<112> (brass texture), {112}<11$\bar{1}$>(copper texture), {123}<634> (S texture), and {110}<001> (Goss texture). However, some differences have been observed in the texture characteristics of NC metals compared with their coarse-grained counterparts. Recent experiments have shown that both copper and cube orientations, instead of brass texture, develop in a heavily deformed NC nickel with an initial grain size of ~28 nm [12]. This phenomenon implies the deformation of such metal can not be depicted by a simple combination of the GB-mediated sliding and dislocation-mediated mechanism. Another new texture component of {110}<100> is found in NC Ni-18Fe alloys rolled at room and liquid-nitrogen temperatures, respectively, suggesting the grain growth is accompanied by the dislocation/twin mediated plasticity [13]. In view of the aforementioned discrepant experimental results, it is of significant interest to investigate the texture evolution during plastic deformation of NC metals.

2. EXPERIMENTAL

Fully dense, electrodeposited nc nickel sheets were procured from Goodfellow Inc. The as-received sheets were 200 μm thick with an average grain size of about 20 nm. Two rectangular samples were stacked together and then went through a pair of rolls at room temperature. During such pack rolling processes, the rolling strains ε_{VM} of each sample were calculated by $\varepsilon_{VM}=|2/\sqrt{3}\ (1+\delta)|$, where δ is the rolling reduction. In particular, we will focus on the texture evolutions at the interface R between the two samples and the interface NR between the sample

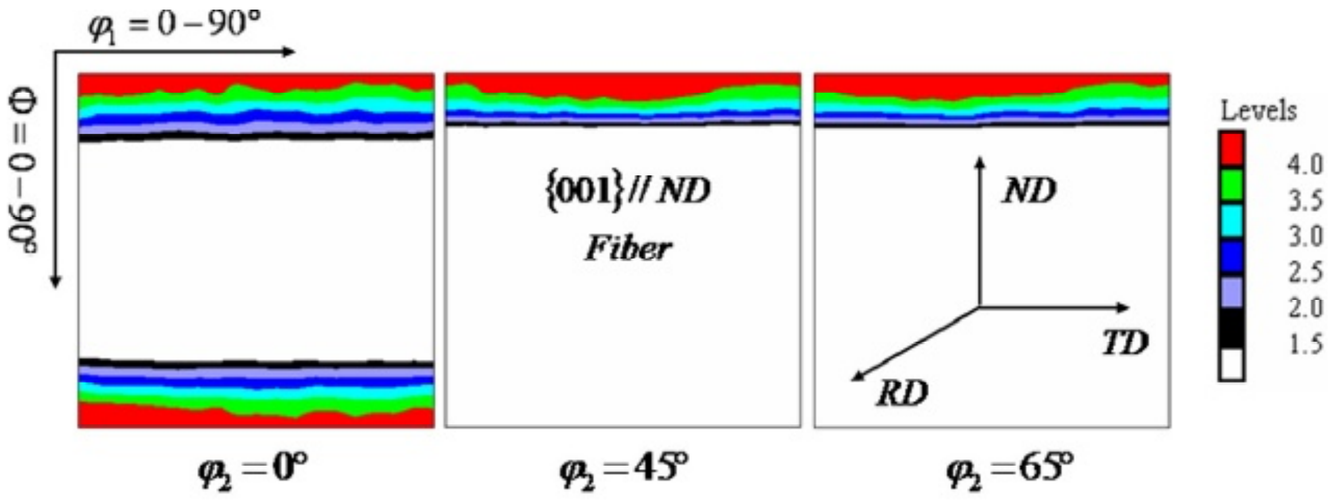

Fig. 2. ODFs for the as received NC nickel sample.

and the roll. A Zeiss Libra 200FE transmission electron microscopy (TEM, operated at 200 kV) was employed to evaluate the microstructure, particularly the grain size distribution for each sample. For the macrotexture measurement on a Rigaku D/max 2500PC X-ray diffractometer (XRD, operated at 40 kV and 150 mA), the samples had a minimum of 1 cm^2 surface area. The (111), (200), (220), and (311) pole figures were measured up to a tilt angle of 70° using the Schultz reflection method with Cu K_α radiation. LaboTex 3.0 software was used for the analysis of the microtexture data. The model functions method is used to quantitatively evaluate the volume fraction of texture components using a 5-degree resolution in the orientation distribution function (ODF) space.

3. RESULTS AND DISCUSSIONS

Fig. 1 displays the results of XRD analysis of both the side NR and side R. Firstly the texture was simply evaluated as the (200)/(111) and (220)/(111) diffraction intensity ratios (I_{200}/I_{111} and I_{220}/I_{111}). These ratios for a complete random orientation in nickel are 0.42 and 0.21 (PDF#04-0850), respectively. It can be seen that a (200) preferred orientation is seen in the as-received sample. Moreover, the different sides exhibit different texture evolutions. Before the strain reaches about 0.30, the (200) preferred orientation strengthens. However, when the strain exceeds about 0.30, the strengthened (200) preferred orientation weakens with increasing plastic strain. For side NR, it is most likely that the grain rotation can be easily initiated by the shear stress. In particular, the value of I_{200}/I_{111} for side R is lower than that for side NR, which is partly due to grain orientation shifting to (220) from (200). For side R, beyond a strain of ~0.20, the (220) preferred orientation is observed. Once ε_{VM} exceeds ~0.50, it is found that the measured intensity of (220) reflection is stronger than that of any other reflections from XRD profiles, resulting in the value of I_{220}/I_{111} surpassing that of I_{200}/I_{111}. Detailed texture analysis by pole figures has confirmed that the initial <100> fibre texture changes to {110}<100> texture for side R under large strain conditions. Note that similar (220) preferred orientation strengthens with increasing strain for side NR, notwithstanding the change is not so obvious, ranging from 0.20 to 0.40. These results imply that the plastic deformation seem to be dominated by grain rotation along with some dislocation activities [14].

Furthermore, the texture components are characterized by ODFs. Fig. 2 shows the ODFs ($\varphi_2 = 0°$, 45°, and 65° sections) for the as-received NC nickel. It is found that the starting texture exhibits a fiber texture with the axis of {001} parallel to the *ND*, which is consistent with previous investigations of growth texture for nickel electrodeposits [15]. This fiber is strongly symmetrical and as long as symmetrical slip systems are activated two of the orientations (the cube orientation {001}<100> and the 45°*ND* rotated cube orientation {001}<110>). However, there are some pronounce changes in the texture components as well as texture intensities after pack-rolling deformation. The ODFs of $\varepsilon_{VM} = 0.256$ cold-rolled sample are shown in Fig. 3. An attention is focused on a comparison between side NR and side R. For the both side NR and side R, the orientation distribution consists of a cube texture component in the $\varphi_2 = 0°$ orientation space. As an essential feature, both ODFs have a maximum value in the section $\varphi_2 = 45°$ with an angle $\varphi_1 = 45°$ and $\Phi = 0°$, corresponding to the ideal orientation {001}<0$\bar{1}$0>. The intensity of this fundamental component in side NR is higher than that in the side R. Additionally, there are some major differences in the side R. As can be seen from the $\varphi_2 = 0°$section for side R, {110}<001> develops, which does not appear in the similar location in side NR. Besides, from the $\varphi_2 = 45°$section, {$\bar{1}$12}<$\bar{1}\bar{1}$0> is found in side R. Fig. 4 shows the ODFs of $\varepsilon_{VM} = 0.611$ deformed NC nickel. Also at higher degrees of deformation the same cube texture component is found in side NR. However, for side R, no cube type com-

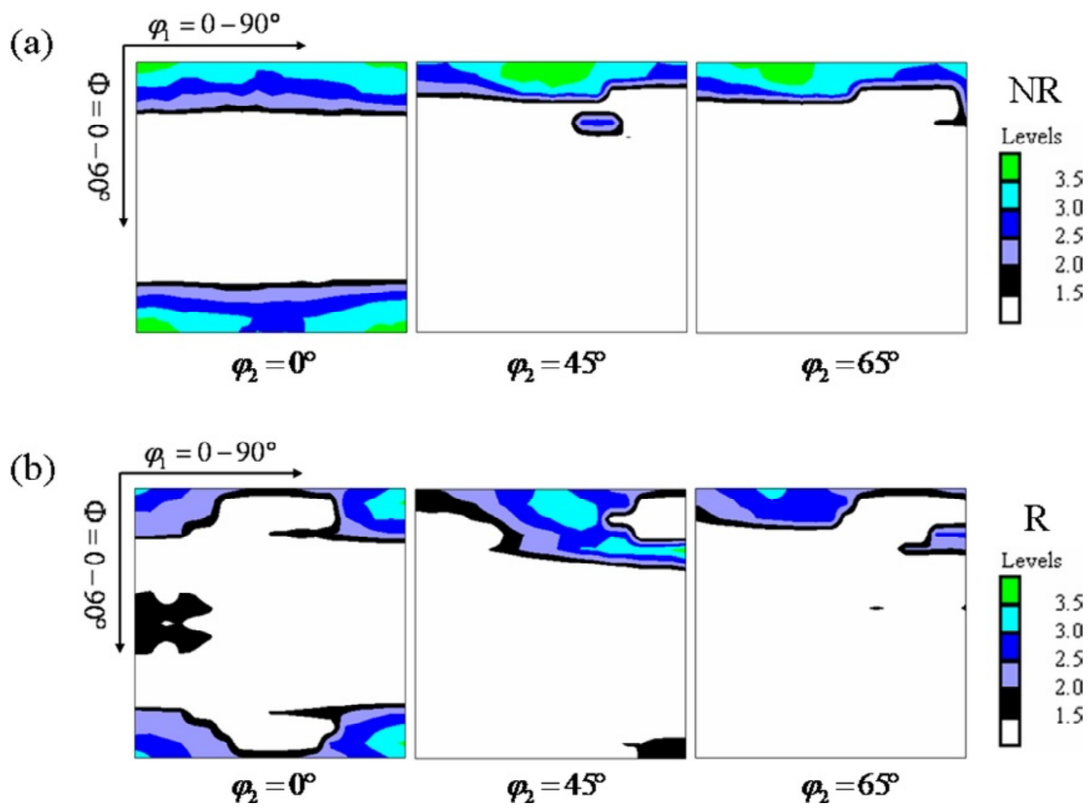

Fig. 3. ODFs for the (a) side NR and (b) side R of NC nickel rolled to ε_{VM}=0.256.

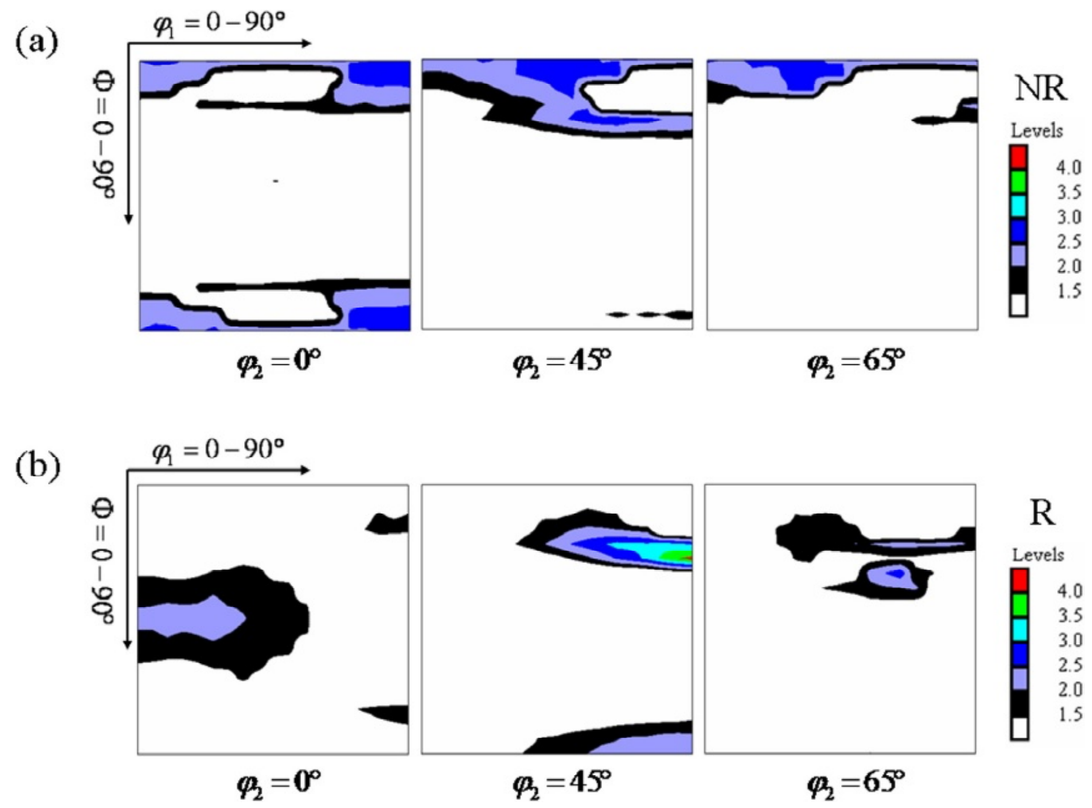

Fig. 4. ODFs for the (a) side NR and (b) side R of NC nickel rolled to ε_{VM}=0.611.

ponents but the goss and brass components are seen from the $\varphi_2 = 0°$section. The $\{\bar{1}12\}\langle\bar{1}\,\bar{1}0\rangle$ component develops and {123}<634> (S texture) is seen in side R.

To better understand the texture evolution during pack rolling of NC nickels, the volume fractions of seven selected texture component are investigated, as shown in Fig. 5. For reference, the {001} fiber in the as-received sample is divided into two orientation ranges, namely {001}<100> and {001}<110>. Quantitative texture analysis shows that the volume fractions of {001}<100> and {001}<110> are 20% and 18%, respectively. After a strain of ε_{VM}=0.087, there is just a small change in these two components. However, for both side NR and side R, the {001}<100> and {001}<110> components significantly decrease with further increasing strain, particularly in the side R. In case of {001}<100> texture, for the ε_{VM}=0.611 sample, the volume fraction is 8% in side NR, while only 2% in side R. This is somewhat different from a reported result that cube texture is enhanced in rolled NC nickel [12]. Instead, this phenomenon is typically found in the cold rolling of conventional FCC metals that cube texture reduces while other rolling texture components become stronger [16]. Another different texture feature in the side NR and R also involves other texture components including $\{110\}\langle1\bar{1}2\rangle$, {110}<001>, {112}<110>, $\{112\}\langle11\bar{1}\rangle$, and {123}<634>. For both the side NR and the side R, the volume fraction of each texture component increases. Especially, the volume fraction of {110}<001> component in the side R of ε_{VM}=0.611 sample reaches 15%, which is larger than that in the side NR. This trend is rather obvious from the analysis of Fig. 4. Although the volume fraction of {110}<001> component is determined to about 5%, it is not seen in the $\varphi_2 = 0°$ section. Additionally, similar trend is also observed in the case of $\{110\}\langle1\bar{1}2\rangle$, {112}<110> and {123}<634> components.

It is well established that the texture development is governed by different deformation modes or

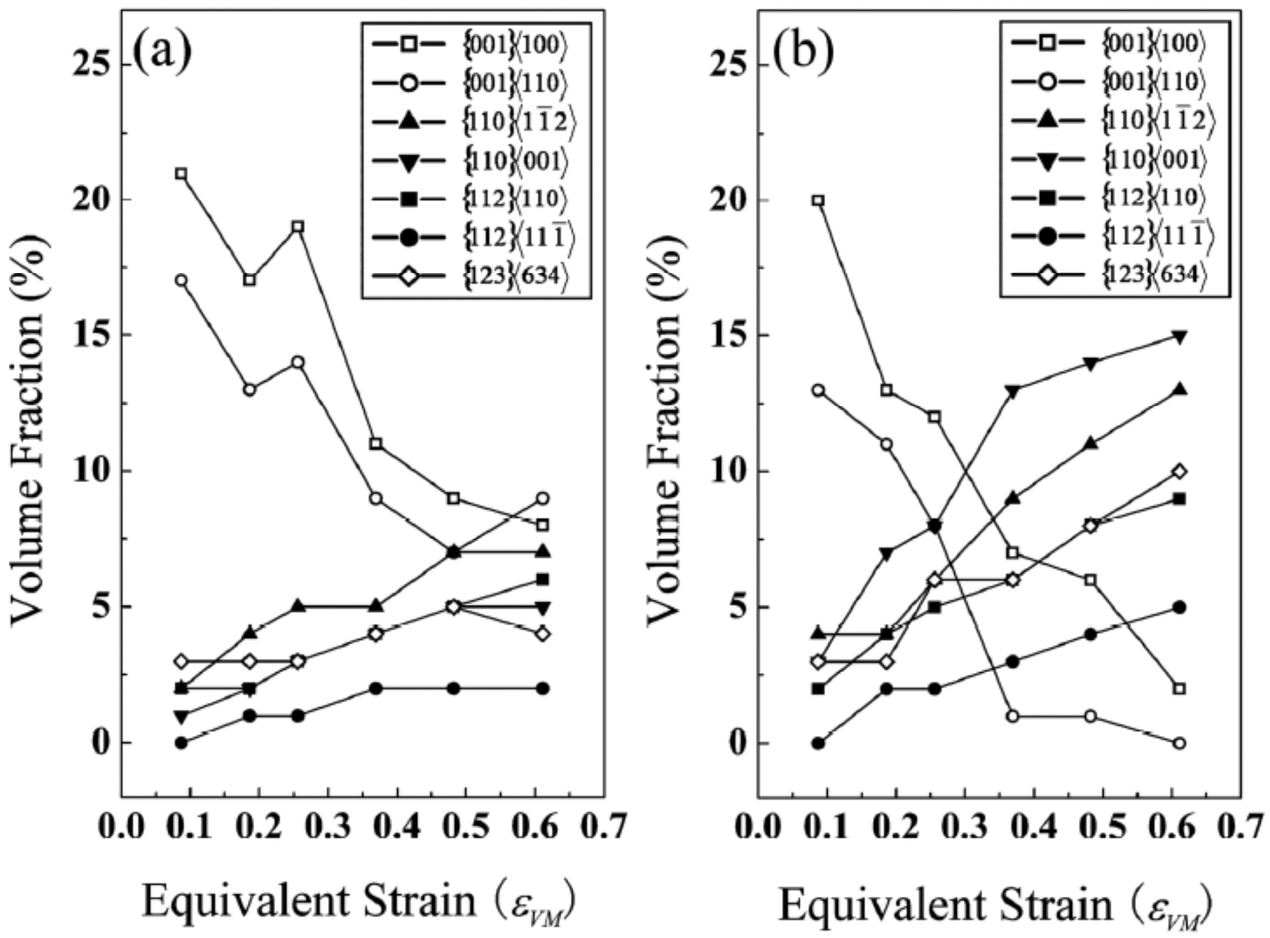

Fig. 5. Volume fractions of seven selected texture component in (a) side NR and (b) side R for deformed NC nickel rolled to different equivalent strains.

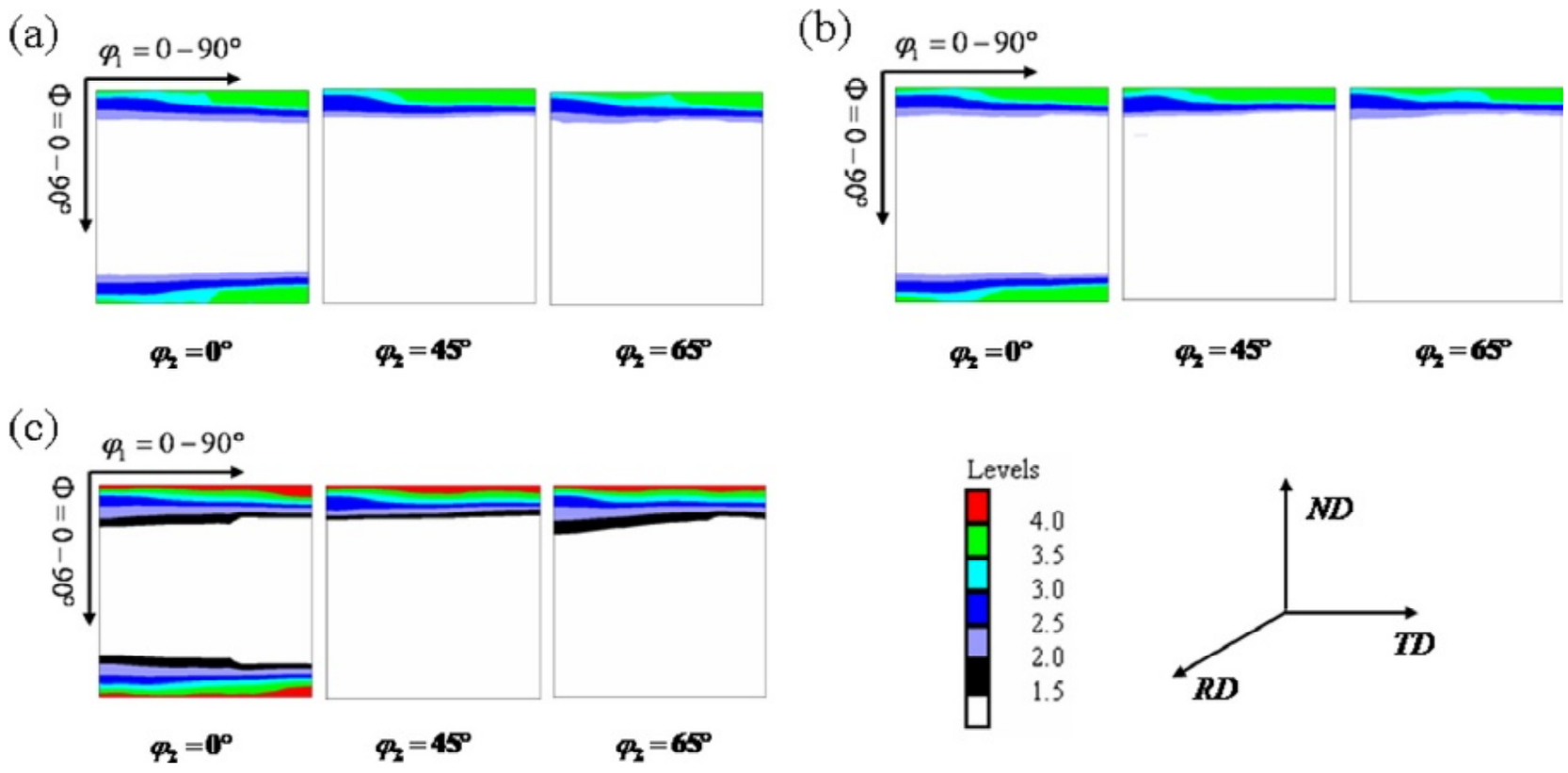

Fig. 6. ODFs for the conventionally rolled NC nickel: (a) $\varepsilon_{VM} = 0.10$, (b) $\varepsilon_{VM} = 0.20$, and (c) $\varepsilon_{VM} = 0.35$.

conditions. From a purely deformation mechanistic point of view, the deformation of NC metal is complex. As mentioned previously, Yang et al. have observed that the cube texture component of the deformation texture is still quite strong after 50% reduction in thickness [12]. Further simulations of this texture evolution have been preformed by adding a shearing-strain component and reducing the number of active {111}<110> slip systems and showed good agreement with experimental data. In considering this discrepancy result from our data, it should be pointed out that the initial thickness and mean grain size of their sample sheets are 0.5 mm and ~28 nm, respectively. Therefore, it is in our interest if the grain size reduce to ~20 nm. Additionally, in the present investigation, we also note that the change in the volume fraction of cube texture components could be divided into two stages according to the equivalent strain: first decreases before the strain of about 0.35 and then gradually changes little once ε_{VM} exceeds 0.35. Thus, a sample of similar dimension was cold rolled in the conventional way and the texture evolution was also compared, as shown in Fig. 6. It can be seen that there is no major change in the textural components as well as texture intensity during conventional cold rolling, although grain rotation indeed takes place in the early stage of rolling as reported in our previous investigation [17]. Moreover, we also note that the grain size reach ~30 nm after $\varepsilon_{VM} = 0.35$ deformation.

To further our understanding of the effect of strain-stress state on texture evolution in plastically deformed nc nickel, we have examined coarse-grained nickel control samples in two different strain-stress conditions. The first is uniaxial compressed and the

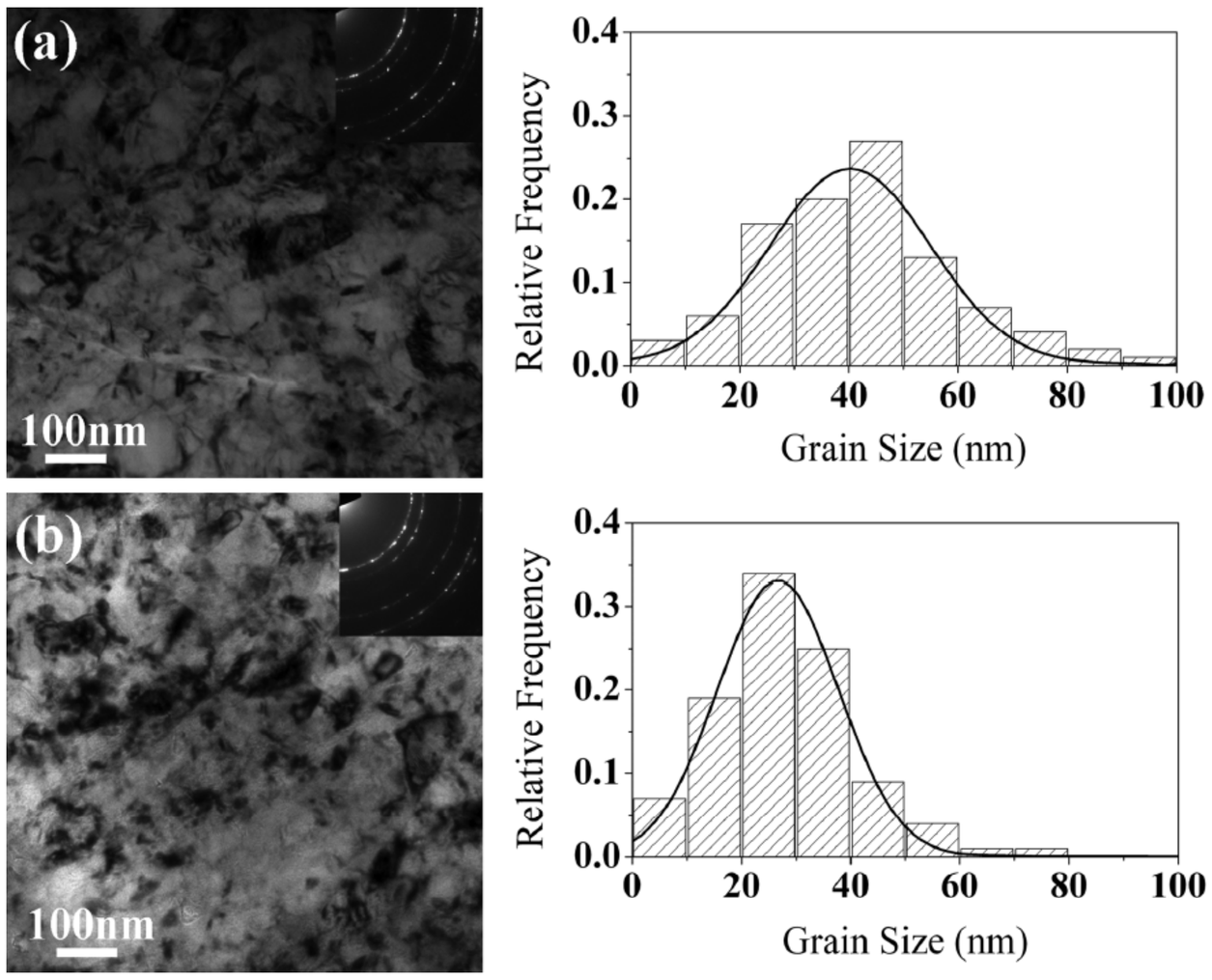

Fig. 7. TEM observations of the typical microstructure for (a) side NR and (b) side R of the $\varepsilon_{VM} = 0.611$ sample show that the grains exhibit an equiaxed morphology. The statistical distributions of grain-size were obtained from corresponding dark-field TEM images of the same samples.

second is deformed by cold rolling. In the case of uniaxial compression, remarkable (220) preferred orientation has been detected. On the contrary, there is an obvious change in (200) orientation in the cold-rolled sample. As a consequence, it has been suggested that the development of {110}<100> texture may be dominated by the uniaxial compressive stress [18,19]. During the pack rolling, for the side NR, the sample simultaneously undergoes compression and shear deformation. Compared to the side R, this may increase the local strain in the side NR above the nominal strain corresponding to the thickness reduction. Particularly in the case of shear deformation, the grains are subjected to a shear stress and this shear stress can further promote dislocation emission during straining and activate new dislocation sources as well. A nature concern arises regarding the grain growth by the grain boundary migration and dislocation activities. As a result, we also observe some discrepancies in grain size change between side NR and side R at a given rolling strain. Take the $\varepsilon_{VM} = 0.611$ deformed sample as an example, typical bright-field TEM images of side NR and side R are shown in Figs. 7a and 7b. It can be seen that grain shapes remain equiaxed after deformation. The corresponding grain-size distribution based on TEM observations indicates that most grains in side NR have a size ranging from 20 nm to 60 nm, while 10 nm to 40 nm in side R. The fact that the grain size in side NR increases faster than that in side R provides an important clue as to the question of texture evolution. Similar to conventional FCC metals, we hold the view that such texture evolutions are still driven by dislocation slip.

Based on the above information, it is likely that dislocation activities play an important role during deformation in addition to the orientation-dependent grain growth. As expected, in the early stage of deformation (before a strain of about 0.35), with strengthened (200) preferred orientation caused by grain rotation, the dislocation generation and slip is the underlying necessity for deformation. It is evident that the volume fraction of cube component decreases largely, but other rolling texture components gradually become stronger. Furthermore, it should be also noted that the grain growth occurs as the result of grain boundary migration, involving relaxation processes of grain boundary structure [20]. Especially for side NR, the shear induce grain growth is one of the most prominent characteristic. Analogous to the annealing process, such grain boundary relaxation could also make it considerably more difficult for grain boundary emission of dislocations [21]. After further deformation above ^ÿ0.35, (200) preferred orientation begins to decrease (Fig. 1), and the dislocation activity and grain rotation become difficult. There is only a small change in volume fraction of each texture component as the deformation continued. On the other hand, it has been suggested that there exists slip-twinning transition in metals and slip is more frequent than twinning [22]. For nc nickel, inverse grain size effect on deformation twinning indicates that deformation twins tend to form in large grains (around 35 nm for rolling deforma-

tion) [23]. In other words, with increasing grain size, it is easier for grains to deform by twinning than slip. For side NR, it has been revealed that about 65 percent of the grains grow up to the size of above 35 nm (Fig. 7a). During deformation, it is reasonable to anticipate that the twins tend to occur more frequently and to be more pronounced in these grains with larger size. Since dislocation slip is greatly suppressed, a remnant of the original cube component can be still observed, as shown in Fig. 4a. However, for side R, the amount of grain growth is limited. Since the deformation of grains is governed mainly by partial dislocation slip, it can be seen that a large decrease in the volume fraction of cube component and even disappear in the final deformed samples (Fig. 5b).

4. CONCLUSIONS

In summary, the texture evolution of NC nickel with an initial grain size of about 20nm during pack rolling at room temperature has been investigated. For both the roll-bonding side and non-roll-bonding side, the volume fractions of {001}<100> and {001}<110> components decrease with increasing equivalent strain, whereas those of {110}<001>, {110}<1$\bar{1}$2>, {112}<110>, and {123}<634> components increase. However, the roll-bonding side and the non-roll-bonding side behave quite differently. The deformation texture in the roll-bonding side at high strain is characterized by the presence of strong {110}<001>, {110}<1$\bar{1}$2>, {112}<110>, and {123}<634> components, whereas a significantly decrease in the {001}<100> and {001}<110> components. A cubic component having a volume fraction of 8% remains found in the non-roll-bonding side for sample deformed to the largest strain of ε_{VM}=0.611. Such texture evolution is still similar as compared to its coarse-grained counterpart, which is driven by dislocation slip.

ACKNOWLEDGEMENTS

We would like to thank W.H. Yin and Q. Wei, from the University of North Carolina at Charlotte, for helpful discussions. This work was supported by the National Natural Science Foundation of China under Grant Nos. 51271208 and the Local Fund for Chongqing University of Arts and Sciences under Grant No. R2012CH09.

REFERENCES

[1] V. Yamakov, D. Wolf, S.R. Phillpot, A.K. Mukherjee and H. Gleiter // *Nat. Mater.* **3** (2004) 43.
[2] M. A. Meyers, A. Mishra and D. J. Benson // *Prog. Mater. Sci.* **51** (2006) 427.
[3] D. Jang and M. Atzmon // *J. Appl. Phys.* **93** (2003) 9282.
[4] H. Conrad // *Mater. Sci. Eng. A* **341** (2003) 216.
[5] Z. W. Shan, E. A. Stach, J. M. K. Wiezorek, J. A. Knapp, D. M. Follstaedt and S. X. Mao // *Science* **305** (2004) 654.
[6] H. Q. Li, P. K. Liaw, H. Choo and A. Misra // *Appl. Phys. Lett.* **93** (2008) 051907.
[7] D. V. Wilson and J. A. Chapman // *Philos. Mag. A* **8** (1963) 1543.
[8] E. Smith and P. J. Worthington // *Philos. Mag. A* **9** (1964) 211.
[9] E. Ma // *Science* **305** (2004) 623.
[10] B. Chen, K. Lutker, S.V. Raju, J. Yan, W. Kanitpanyacharoen, J. Lei, S. Yang, H.R. Wenk, H.K. Mao and Q. Williams // *Science* **338** (2012) 1448.
[11] S. Scheriau and R. Pippan // *Mater. Sci. Eng. A* **493** (2008) 48.
[12] Y. L. Yang, N. Jia, Y. D. Wang, Y. F. Shen, H. Choo and P. K. Liaw // *Mater. Sci. Eng. A* **493** (2008) 86.
[13] P.K. Liaw, L. Li, T. Ungar, Y.D. Wang, J.R. Morris, G. Tichy, J. Lendvai, Y.L. Yang, Y. Ren and H. Choo // *Acta Mater.* **57** (2009) 4988.
[14] B. B. Rath, M. Winning and J. C. M. Li // *Appl. Phys. Lett*. **90** (2007) 161915.
[15] C. B. Nielsen, A. Horsewell and M.J.L. Ostergard // *J. Appl. Electrochem*. **27** (1997) 839.
[16] B. Verlinden, I. Samajdar, L. Rabet and P. Van Houtte // *Mater. Sci. Eng. A* **266** (1999) 146.
[17] X.Y. Zhang, Q. Liu, X.L. Wu and A.W. Zhu // *Appl. Phys. Lett.* **93** (2008) 261907.
[18] H. Garmestani, S. Lin, B. L. Adams and S. Ahzi // *J. Mech. Phys. Solids* **49** (2001) 589.
[19] G. Y. Chin // *Metall. Trans*. **4** (1973) 329.
[20] A. J. Haslam, S. R. Phillpot, H. Wolf, D. Moldovan and H. Gleiter // *Mater. Sci. Eng. A* **318** (2001) 293.
[21] L. Lu, N. R. Tao, L. B. Wang, B. Z. Ding and K. Lu // *J. Appl. Phys.* **89** (2001) 6408.
[22] M. A. Meyers, O. Vohringer and V. A. Lubarda // *Acta Mater*. **49** (2001) 4025.
[23] X. L. Wu and Y. T. Zhu // *Phys. Rev. Lett.* **101** (2008) 025503.